



Constitutive EGFR Activation Induced by PTPRR Downregulation Confers Resistance to KRAS Inhibitors

Hiroaki Kanemura¹, Toshiyuki Takehara², Osamu Maenishi³, Shuta Tomida⁴, Natsumi Iwawaki², Kei Kunimasa⁵, Tomohiro Nakayama⁶, Satomi Watanabe⁶, Shinichiro Suzuki¹, Kazuko Sakai^{7,8}, Koichi Azuma⁹, Keita Kudo¹⁰, Kazuto Nishio^{7,8}, Kazuhiko Nakagawa¹, Hidetoshi Hayashi¹, Takeshi Teramura², and Kimio Yonesaka¹

ABSTRACT

KRAS^{G12C} inhibitors, such as sotorasib, show clinical efficacy for non-small cell lung cancer (NSCLC) positive for the G12C mutations of KRAS, but primary and acquired resistance to these drugs remains a clinical problem. In this study, we show that the development of resistance to sotorasib in KRAS^{G12C}-positive NSCLC cells was mediated by constitutive activation of EGFR resulting from downregulation of the protein tyrosine phosphatase receptor type R (PTPRR). PTPRR has been identified as a physiologic regulator of ERK signaling in several cancer types. In our study, PTPRR was demonstrated to bind directly to EGFR, facilitating its dephosphorylation on tyrosine residues. Resumption of PTPRR expression in the resistant cells attenuated EGFR phosphorylation and restored sotorasib sensitivity. PTPRR downregulation was associated with gene promoter hypermethylation in the sotorasib-resistant cells and NSCLC tissue samples. Furthermore, low PTPRR expression in tumor specimens was associated with shorter progression-free and

overall survival for patients with NSCLC treated with sotorasib. In contrast to sotorasib, high PTPRR expression was associated with a poor response to EGFR tyrosine kinase inhibitors in EGFR-mutated NSCLC, suggesting that PTPRR may broadly regulate EGFR dependence in NSCLC. Finally, dual blockade of KRAS^{G12C} and EGFR showed a substantial antitumor effect in a xenograft model of sotorasib-resistant NSCLC. This approach is therefore a rational therapeutic strategy for KRAS^{G12C}-positive NSCLC, especially for tumors showing PTPRR downregulation.

Significance: The current study shows that downregulation of PTPRR induces EGFR activation and resistance to KRAS^{G12C} inhibitors in NSCLC, suggesting dual KRAS-EGFR blockade as a rational therapy. PTPRR may help identify patient subgroups that would benefit from the addition of EGFR inhibitors to KRAS^{G12C}-targeted therapies.

Introduction

The RAS family of proteins comprises KRAS, HRAS, and NRAS and plays a key role in human cancer. Each RAS protein is a small GTPase that serves as a signaling switch and toggles between guanosine triphosphate (GTP)-bound (active) and guanosine diphosphate (GDP)-bound (inactive) states. In its GTP-bound state, RAS activates several downstream effector pathways—including the MAPK and PI3K pathways—and thereby

promotes cell proliferation, migration, and survival (1–4). About 20% of all human malignancies harbor oncogenic mutations of the RAS family of genes, with KRAS alone accounting for 75% of these mutations (5). The most common KRAS mutations affect the glycine-12 residue of the encoded protein, which is replaced by cysteine (KRAS^{G12C}) or aspartate (KRAS^{G12D}). These mutations render the protein insensitive to the stimulatory effect of GTPase-activating protein on GTPase activity and therefore serve to maintain KRAS in the GTP-bound (active) form and

¹Department of Medical Oncology, Kindai University Faculty of Medicine, Sakai, Japan. ²Division of Cell Biology for Regenerative Medicine, Institute of Advanced Clinical Medicine, Kindai University Faculty of Medicine, Sakai, Japan. ³Department of Pathology, Kindai University Faculty of Medicine, Sakai, Japan. ⁴Center for Comprehensive Genomic Medicine, Okayama University Hospital, Okayama, Japan. ⁵Department of Thoracic Oncology, Osaka International Cancer Institute, Osaka, Japan. ⁶Department of Medical Oncology, Kishiwada City Hospital, Kishiwada, Japan. ⁷Department of Genome Biology, Kindai University Faculty of Medicine, Sakai, Japan. ⁸Center for Genomics, Life Science Research Institute, Kindai University, Sakai, Japan. ⁹Division of Respiratory, Neurology, and Rheumatology, Department of Internal Medicine, Kurume University School of Medicine, Kurume, Japan. ¹⁰Department of Medical Oncology, National Hospital Organization Osaka Minami Medical Center, Kawachinagano, Japan.

H. Kanemura and T. Takehara contributed equally to this article.

T. Teramura and K. Yonesaka jointly supervised this work.

Corresponding Authors: Kimio Yonesaka, Department of Medical Oncology, Kindai University Faculty of Medicine, 1-14-1 Mihara-dai, Minami-ku, Sakai 590-0197, Japan. E-mail: yonesaka@med.kindai.ac.jp; and Takeshi Teramura, Division of Cell Biology for Regenerative Medicine, Institute of Advanced Clinical Medicine, Kindai University Faculty of Medicine, 1-14-1 Mihara-dai, Minami-ku, Sakai 590-0197, Japan. E-mail: teramura@med.kindai.ac.jp

doi: 10.1158/2767-9764.CRC-25-0489

This open access article is distributed under the Creative Commons Attribution 4.0 International (CC BY 4.0) license.

©2026 The Authors; Published by the American Association for Cancer Research

to activate downstream signaling pathways that promote tumor cell growth (1–4).

The KRAS^{G12C} mutation has been detected in lung adenocarcinoma (14%), colorectal cancer (5%), and pancreatic tumors (1%; ref. 6). The first clinically available KRAS^{G12C} inhibitors, sotorasib and adagrasib, have been shown to have a 30% to 40% response rate and to give rise to a progression-free survival (PFS) of ~6 months in individuals with KRAS^{G12C}-positive non-small cell lung cancer (NSCLC; refs. 4, 7–9). These agents bind to an allosteric pocket near the mutant cysteine residue that has been designated the switch II pocket (2). These inhibitors require this cysteine residue for binding and suppress KRAS^{G12C} signaling and tumor cell growth by binding covalently and selectively to KRAS^{G12C}-GDP (10). Although these compounds have improved treatment outcomes for individuals with KRAS^{G12C}-positive NSCLC, the extent and duration of their effects are limited compared with those of EGFR and ALK inhibitors, which typically achieve response rates of ~70% and ~80% and a median PFS of 18.9 and 34.8 months, respectively (11–13). Furthermore, the response rates of these inhibitors in colorectal cancer and pancreatic ductal adenocarcinoma are only ~10% to 30%, further indicative of the inadequacy of their therapeutic effects (14–16).

Concurrent mutations of *KEAP1*, *SMARCA4*, and *CDKN2A* have been identified as key drivers of early disease progression in patients treated with single-agent sotorasib or adagrasib (17). On-treatment feedback reactivation of the RAS-MAPK pathway, resulting from the new synthesis and GTP loading of KRAS^{G12C} or RTK-mediated activation of wild-type RAS, can compromise the clinical efficacy of KRAS^{G12C} inhibitors (18). In addition, secondary genetic alterations of RAS-MAPK pathway components, which often emerge in multiple genes simultaneously as a result of convergent tumor evolution, or transdifferentiation of adenocarcinoma into squamous histology can further drive disease progression and present additional challenges to the improvement of clinical outcomes (19–22). The high prevalence of primary and acquired resistance to KRAS^{G12C} inhibitors has led to the development of numerous combinations of these agents with other drugs that are being evaluated in clinical trials for their ability to overcome therapy resistance (23).

We here show that the expression of protein tyrosine phosphatase (PTP) receptor type R (PTPRR) was downregulated via methylation of its gene promoter in sotorasib-resistant cancer cells. This downregulation of PTPRR resulted in the activation of EGFR–MAPK (ERK) signaling and thereby conferred sotorasib resistance. We also show that dual blockade of KRAS^{G12C} and EGFR is a rational therapeutic strategy for KRAS^{G12C}-positive cancer with reduced expression of PTPRR.

Materials and Methods

Cell culture and reagents

The KRAS^{G12C}-mutant NSCLC cell lines NCI-H2122 (RRID: CVCL_1531), SW1573 (RRID: CVCL_1720), and NCI-H358 (RRID: CVCL_1559); the EGFR-mutated NSCLC cell line NCI-H1975 (RRID: CVCL_1511); and the KRAS^{G12C}-mutant colorectal cancer cell line SW837 (RRID: CVCL_1729) were obtained from the ATCC. The authenticity of the cell lines was confirmed by short tandem repeat profiling in May 2021. All cell lines were regularly tested for *Mycoplasma* contamination using the MycoAlert Mycoplasma Detection Kit (Lonza), and the most recent test confirmed that the

cell lines were *Mycoplasma*-free in November 2025. H2122, SW1573, H358, H1975, and SW837 cells were cultured under a humidified atmosphere of 5% CO₂ at 37°C in RPMI 1640 (Sigma-Aldrich) supplemented with 10% FBS and 1% penicillin-streptomycin. Sotorasib, adagrasib and osimertinib were obtained from MedChemExpress, and cetuximab was from Bristol Myers Squibb.

Cell viability assay

Cell viability was assessed with a CellTiter-Glo luminescence assay (cat. #G7571, Promega). Cells were seeded in 96-well round-bottom plates at a density of 2×10^3 /well, cultured for 24 hours, and then exposed to drugs for 72 hours before the assay. Luminescence was measured with a microplate reader (ARVO MX1420; PerkinElmer), and values were expressed as a percentage of that for untreated cells.

Immunoblot analysis

Cells (1×10^6 to 1×10^7) were seeded in 90-mm PrimeSurface plates (Sumitomo Bakelite) and incubated overnight in RPMI 1640 supplemented with 2% FBS or treated with drugs as indicated before analysis. Immunoblot analysis was performed as described previously (24). The primary antibodies used are listed in Supplementary Table S1.

Reverse transcription-quantitative PCR analysis

Total RNA was extracted from cells using the TRIzol reagent (Thermo Fisher Scientific) and was subjected to reverse transcription (RT) with a PrimeScript RT Master Mix Kit (Takara Bio). The resulting cDNA was subjected to real-time PCR analysis with Perfect Real-Time SYBR Green II (Takara Bio) and a Thermal Cycler Dice Real-Time System Single (Takara Bio). The protocol consisted of incubation at 95°C for 20 seconds, followed by 40 cycles of 95°C for 5 seconds and 60°C for 30 seconds. For quantitation of relative gene expression, the threshold cycle values were normalized by that for the housekeeping gene *GAPDH* and were then calibrated with the $\Delta\Delta C_t$ method. Amplification of contaminating genomic DNA was limited by the use of primers designed to span at least one intron. Primer sequences are provided in Supplementary Table S2.

Coimmunoprecipitation analysis

Cells were lysed in immunoprecipitation extraction buffer [25 mmol/L Tris-HCl (pH 7.5), 100 mmol/L NaCl, 0.5% Triton X-100] for 30 minutes on ice. The lysate was centrifuged to remove debris, and the resulting supernatant was incubated overnight at 4°C with primary antibodies conjugated to Dynabeads Protein G (Thermo Fisher Scientific) in Tris-buffered saline containing 0.02% Tween-20. The precipitated proteins were eluted from the beads with SDS sample buffer for immunoblot analysis. All antibodies used are listed in Supplementary Table S1.

siRNA transfection

Cells were seeded at 50% to 60% confluency in 12-well plates and cultured for 24 hours before transient transfection for 72 hours with siRNAs mixed with the Lipofectamine RNAiMax reagent (Thermo Fisher Scientific). The cells were then transferred to six-well plates for immunoblot analysis or to 96-well plates for growth inhibition assays. A scrambled control siRNA and PTPRR-specific siRNAs (Supplementary Table S2) were obtained from Japan Bio Services.

Establishment of PTPRR-overexpressing cell lines

The pPB[Exp]-Puro-CAG-3xFLAG/PTPRR[NM_001207016.1]-IRES-EGFP (VectorBuilder Inc.) vector or the pPB-CAG-EGFP-IRES-Puro vector was transfected into H2122 and H2122AR30 cells together with a plasmid encoding the piggyBac transposase using a NEPA21 electroporation system (Nepa Gene). These cells were cultured in DMEM supplemented with 10% FBS and puromycin (1 ng/mL) for 10 days.

Colony formation assay

H2122 and H2122AR30 cells were seeded at a density of 1×10^3 per well in six-well plates, cultured for 24 hours, and then treated with 1 μ mol/L sotorasib, cetuximab (10 μ g/mL), or both drugs for 28 days, with replacement of the medium every 3 days. The cells were then gently washed with PBS, fixed with acetic acid/methanol (1:7 vol/vol) for 5 minutes, washed again, and stained with 0.5% crystal violet for 2 hours at room temperature.

Bisulfite sequencing

Genomic DNA was isolated from cells using a Quick-DNA Miniprep Plus Kit (Zymo Research) and from formalin-fixed, paraffin-embedded (FFPE) tumor specimens using an AllPrep DNA/RNA FFPE Kit (QIAGEN). The quality and quantity of the isolated DNA were determined using a NanoDrop 2000 device (Thermo Fisher Scientific) and a PicoGreen dsDNA Assay Kit (Thermo Fisher Scientific), respectively. The DNA was processed with an EpiTect Fast DNA Bisulfite Kit (QIAGEN), and the target *PTPRR* sequence in the samples obtained after bisulfite treatment was amplified by PCR using Takara EpiTaq HS (Takara Bio) and a Thermal Cycler Dice instrument (Takara Bio) with the primers (forward and reverse, respectively) 5'-TGAATTAGGTAGTTTTTAAGAGAGA-3' and 5'-TAAAATCCTTCTTACTCCAAATTTTAT-3'. The incubation protocol comprised an initial incubation for 2 minutes at 95°C; 45 cycles of 20 seconds at 95°C, 30 seconds at 53°C, and 20 seconds at 72°C; and a final incubation for 5 minutes at 72°C. The PCR products were then used as templates. The sequencing primer hybridized close to the sequence of interest. Pyrosequencing was performed using PyroMark Gold Q24 reagents (QIAGEN) and a PyroMark Q24 instrument (QIAGEN). The resulting pyrogram was analyzed with pyrosequencing data analysis software (QIAGEN).

Cell line-derived xenograft models

All animal experiments were approved by the Committee on Safety and Ethical Handling Regulations for Laboratory Animal Experiments of Kindai University and were performed in accordance with institutional guidelines. H2122 or H2122AR30 cells (5×10^6) were injected subcutaneously into the right flank of 4- to 6-week-old male BALB/cA|cl-nu/nu mice (CLEA Japan). After the tumors had achieved a volume of 0.2 cm³, the mice were randomly assigned to treatment and control groups. The animals were treated orally with sotorasib (100 mg/kg per day) or intraperitoneally with cetuximab (40 mg/kg twice weekly). Tumor volume and body weight were measured twice weekly in a nonblinded manner. The mice were killed if the tumors became necrotic or grew to a volume of 3 cm³. Tumor volume was defined as follows: $0.5 \times \text{length} \times \text{width}^2$.

Tumor specimens and clinical data

FFPE tissue specimens were obtained from individuals with NSCLC with *EGFR* activating mutations or KRAS^{G12C} who were treated at Kindai

University Hospital, Kishiwada City Hospital, Izumi City General Hospital, or Osaka International Cancer Institute between 2018 and 2024. Most of the tumor specimens were collected from the lung during a bronchoscopic diagnostic biopsy or surgical resection. Clinical data were retrieved from the medical records of the patients. Overall survival (OS) was measured from treatment initiation to death from any cause, whereas PFS was measured from treatment initiation to clinical or radiographic progression or death.

IHC staining

FFPE tissue sections (thickness of 4 μ m) were depleted of paraffin, subjected to antigen retrieval by treatment with trypsin, and stained with antibodies to PTPRR (17937-1-AP; Proteintech) as previously described (25). Given that IHC has shown that PTPRR is present mostly in the cytoplasm and that its staining varies in intensity, we performed a quantitative analysis of PTPRR expression in tumor cells according to the methodology adopted for similar molecular staining patterns in previous studies (26). No staining in 100% of cells was defined as negative status. Weak, regardless of the percentage of positive cells, or strong cytoplasmic reactivity in <50% of cells was defined as low, and strong cytoplasmic reactivity in >50% of cells was defined as high. The expression of PTPRR in cancer cells was interpreted by a board-certified pathologist in a blinded manner.

Statistical analysis

Comparisons of continuous variables between two groups were performed using the unpaired *t* test unless indicated otherwise, and those among more than two groups were performed with one-way ANOVA followed by Dunnett's multiple comparison test. Differences in survival curves constructed by the Kaplan–Meier method were assessed with the log-rank test. Missing data were not imputed. All *P* values are based on a two-sided hypothesis. Statistical analysis was performed with Stata IC software version 14.2 (RRID: SCR_012763, StataCorp), and data were graphically depicted using Stata IC version 14.2 and GraphPad Prism 7.0 (RRID: SCR_002798, GraphPad Software). A *P* value of < 0.05 was considered statistically significant.

Study approval

All animal experiments were performed in accordance with the Recommendations for the Handling of Laboratory Animals for Biomedical Research and in compliance with the Committee on Safety and Ethical Handling Regulations for Laboratory Animal Experiments of Kindai University. The analysis of human specimens was also conducted in accordance with the Declaration of Helsinki and was approved by the Institutional Review Boards of the participating facilities. Written informed consent was obtained from all participants after an opportunity to opt out of this study was provided.

Results

EGFR plays a pivotal role in resistance to sotorasib in KRAS^{G12C}-positive NSCLC cells

To explore the mechanisms of sotorasib resistance, we generated resistant clones of KRAS^{G12C}-mutant NSCLC (H2122) cells by exposing the parental cells to increasing concentrations of sotorasib over 10 months, as previously described (24). Whereas sotorasib exposure reduced the viability of parental H2122 cells in a concentration-dependent manner, the sotorasib-resistant clones—designated H2122AR14 and H2122AR30—remained viable in the

presence of 1 μmol/L sotorasib (Fig. 1A). The IC₅₀ of H2122AR14 (4.34 μmol/L) and H2122AR30 (4.79 μmol/L) cells was thus greater than that of the parental cells (0.05 μmol/L). Similar results were obtained with the KRAS^{G12C} inhibitor adagrasib, with the IC₅₀ values of this drug being 0.03 μmol/L for parental H2122 cells and 9.35 μmol/L for H2122AR30 cells (Supplementary Fig. S1).

We next examined intracellular signaling in the KRAS^{G12C}-mutant cells exposed to 1 μmol/L sotorasib (Fig. 1B). Immunoblot analysis revealed that sotorasib induced an upward shift of the KRAS band, reflecting the conversion of the GTP-bound (active) form to the GDP-bound (inactive) form, in both parental and sotorasib-resistant H2122 cells. These results thus suggested that sotorasib maintains KRAS^{G12C} in the inactive form in sotorasib-resistant H2122AR14 and H2122AR30 cells as well as in parental H2122 cells. Sotorasib also reduced the phosphorylation level of ERK but not that of AKT in the parental cells, indicating that sotorasib inhibited ERK signaling. However, sotorasib did not affect ERK phosphorylation in H2122AR14 or H2122AR30 cells.

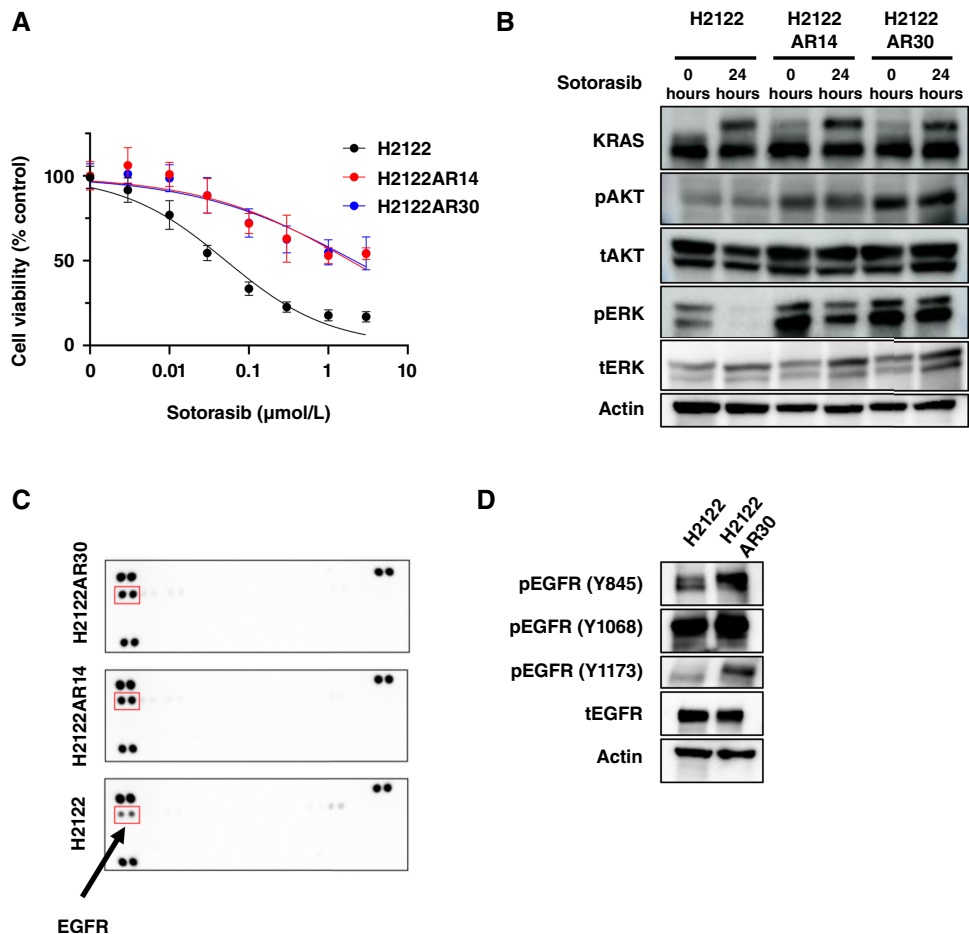
Secondary alterations in on- or off-target genes in KRAS^{G12C}-positive cancer cells have previously been shown to result in resistance to sotorasib through activation of ERK signaling (19, 21, 27). However, a next-generation sequencing panel detected no secondary gene alterations related to sotorasib resistance in sotorasib-resistant H2122AR14 or H2122AR30 cells (Supplementary Table S3),

suggestive of a nongenetic mechanism of acquired resistance to sotorasib. We then assessed the activity of multiple RTKs that potentially activate ERK signaling using a human phospho-RTK array. Among the 49 RTKs examined, phosphorylation of EGFR was increased in H2122AR14 and H2122AR30 cells compared with parental H2122 cells (Fig. 1C). In addition, immunoblot analysis showed that phosphorylation of EGFR, in particular that at Y1173, was increased in H2122AR30 cells compared with the parental cells (Fig. 1D). These results suggested that constitutive activation of EGFR, potentially with contributions from other receptor tyrosine kinases or other signaling factors, may underlie ERK activation in the sotorasib-resistant H2122 cells.

Expression of PTPRR is diminished in sotorasib-resistant cells

To elucidate the molecular context of the increased phosphorylation of EGFR in sotorasib-resistant H2122 cells, we compared gene expression patterns between the resistant clones and the parental cells by microarray analysis. Assuming a shared resistance mechanism for H2122AR14 and H2122AR30 cells, we identified 126 genes with common expression changes in both cell lines (Supplementary Fig. S2). These up- or downregulated genes did not include those for EGFR ligands or other HER (human EGFR) family members. However, the gene for PTPRR was downregulated in the resistant clones relative to the parental cells (Fig. 2A and B; Supplementary Table S4).

FIGURE 1. H2122AR14 and H2122AR30 cells are resistant to sotorasib *in vitro* and show EGFR activation. **A**, Cell viability assay for KRAS^{G12C}-mutant parental H2122 cells and H2122AR14 and H2122AR30 sotorasib-resistant clones exposed to the indicated concentrations of sotorasib for 72 hours. Data are means ± SD (*n* = 3 independent experiments). **B**, Immunoblot analysis of KRAS, phosphorylated (p) and total (t) forms of AKT and ERK, and actin (loading control) in H2122, H2122AR14, and H2122AR30 cells treated with sotorasib (1 μmol/L) for 0 or 24 hours. **C**, Human phospho-RTK assay for H2122, H2122AR14, and H2122AR30 cells treated with 1 μmol/L sotorasib for 72 hours. **D**, Immunoblot analysis of Y845-, Y1068-, or Y1173-phosphorylated and total forms of EGFR in H2122 and H2122AR30 cells. Data in **B-D** are representative of at least three independent experiments.



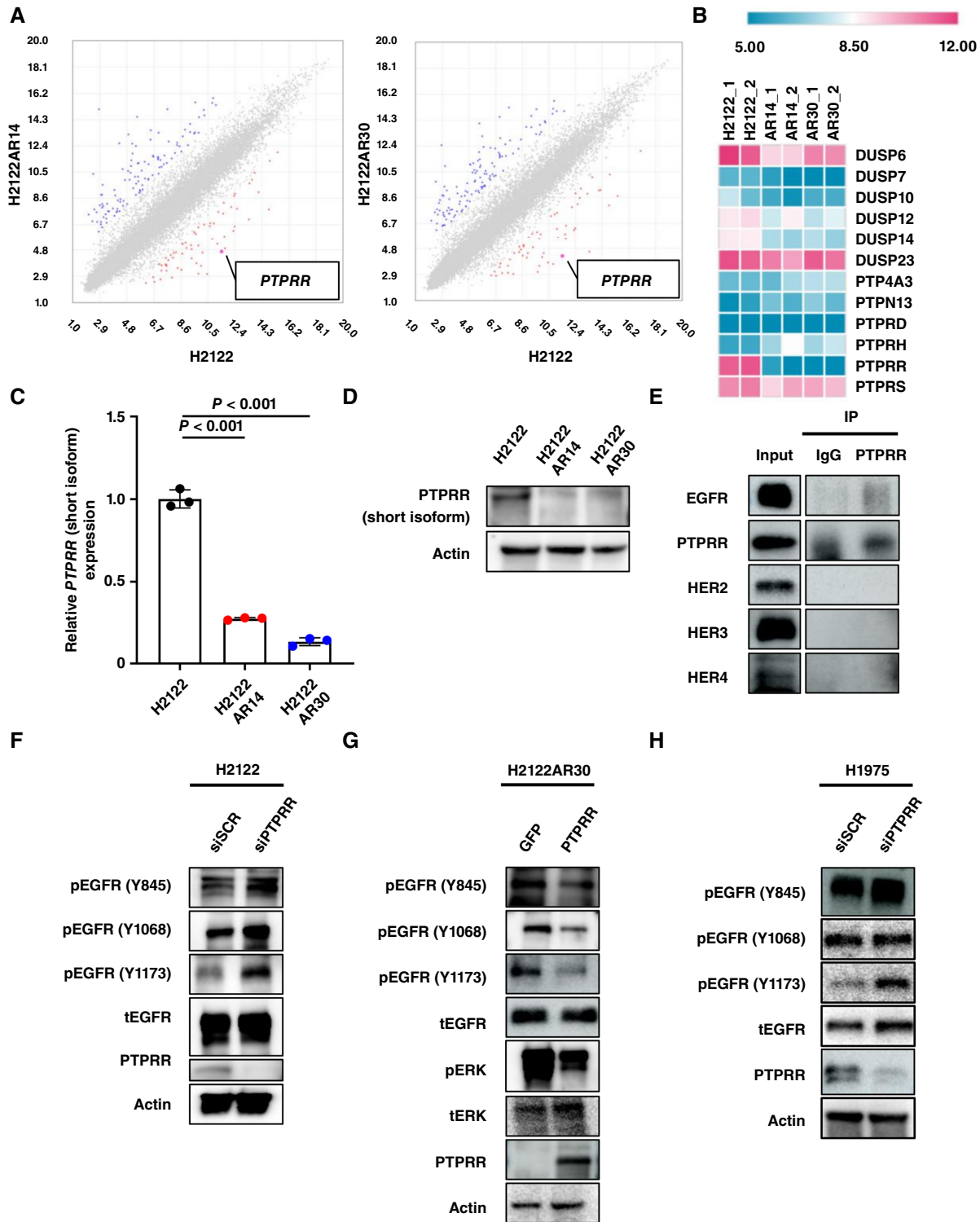


FIGURE 2. PTPRR is downregulated in sotorasib-resistant cells and mediates EGFR dephosphorylation. **A**, Scatter plots of gene expression in H2122 vs. H2122AR14 cells (left) or in H2122 vs. H2122AR30 cells (right) as revealed by microarray analysis. Each axis represents log₂ intensity. Genes that are significantly up- or downregulated more than 10-fold in both sotorasib-resistant clones are shown in red and blue, respectively. **B**, Heatmap for the expression of phosphatase genes in two biological replicates of H2122, H2122AR14, and H2122AR30 cells determined as in **A**. **C**, RT-qPCR analysis of relative *PTPRR* mRNA abundance in H2122, H2122AR14, and H2122AR30 cells. Data are means ± SD (*n* = 3 independent experiments) and were analyzed by one-way ANOVA and Dunnett’s test. **D**, Immunoblot analysis of PTPRR in H2122, H2122AR14, and H2122AR30 cells. **E**, Lysates from H2122 cells transfected with PTPRR expression plasmids were subjected to immunoprecipitation (IP) with (Continued on the following page.)

(Continued) antibodies to PTPRR or with control IgG, and the resulting precipitates as well as the original cell lysates (Input) were subjected to immunoblot analysis with antibodies to either EGFR, PTPRR, HER2, HER3, or HER4. **F**, Immunoblot analysis of PTPRR as well as total and phosphorylated forms of EGFR in H2122 cells transfected with nonspecific control (siSCR) or PTPRR-specific (siPTPRR) siRNAs. **G**, Immunoblot analysis of PTPRR as well as total and phosphorylated forms of EGFR and ERK in H2122AR30 cells stably transfected with expression vectors for GFP (control) or PTPRR. **H**, Immunoblot analysis of PTPRR as well as total and phosphorylated forms of EGFR, AKT, and ERK in H1975 cells transfected with nonspecific control or PTPRR-specific siRNAs. Data in **D–H** are representative of at least three independent experiments.

PTPRR exists as two major isoforms generated from distinct promoters; in this study, we primarily analyzed the short isoform, which is predominantly expressed in NSCLC. RT-quantitative PCR (RT-qPCR) analysis confirmed that the abundance of *PTPRR* mRNA was reduced in H2122AR14 and H2122AR30 cells compared with the parental cells (Fig. 2C), whereas immunoblot analysis showed that the amount of PTPRR protein was also downregulated in the resistant clones (Fig. 2D).

We next examined the potential functional relation between EGFR and PTPRR by coimmunoprecipitation analysis. Immunoprecipitation with antibodies to PTPRR revealed that PTPRR was associated with EGFR but not with other HER family members in H2122 cells (Fig. 2E). Given that PTPRR dephosphorylates tyrosine residues of substrate proteins, we investigated the effect of PTPRR knockdown by RNAi on the phosphorylation of EGFR in parental H2122 cells. Knockdown of PTPRR increased the phosphorylation of EGFR on tyrosine residues, most prominently at Y1173, whereas it did not affect total EGFR abundance (Fig. 2F). Conversely, overexpression of PTPRR reduced the phosphorylation of EGFR tyrosine residues in H2122AR30 cells (Fig. 2G). We also found that PTPRR knockdown increased tyrosine phosphorylation of EGFR in H1975 NSCLC cells, which harbor an activating mutation of EGFR (Fig. 2H). Collectively, these results suggested that PTPRR binds to EGFR and directly mediates its dephosphorylation at tyrosine residues.

Downregulation of PTPRR confers resistance to sotorasib through activation of EGFR-ERK signaling

To determine whether downregulation of PTPRR induces resistance to sotorasib, we examined sensitivity to the drug in PTPRR-depleted H2122 cells. PTPRR knockdown indeed reduced the sensitivity of these cells to sotorasib, with IC_{50} values of 4.2 and 0.041 $\mu\text{mol/L}$ for the cells transfected with PTPRR and control siRNAs, respectively (Fig. 3A). Knockdown of PTPRR also increased the phosphorylation of AKT and ERK in H2122 cells (Fig. 3B). To assess whether this phenomenon was reproducible in additional KRAS^{G12C}-mutant models, we performed similar experiments with another KRAS^{G12C}-mutant NSCLC cell line (H358) as well as in the KRAS^{G12C}-mutant colorectal cancer cell line SW837. In both H358 and SW837 cells, PTPRR knockdown similarly reduced sensitivity to sotorasib, indicating that PTPRR downregulation-mediated resistance is not restricted to the H2122 background (Supplementary Fig. S3A–S3D).

Sotorasib treatment reduced the phosphorylation of ERK in control cells but not in PTPRR knockdown cells (Fig. 3B). We then examined whether overexpression of PTPRR might restore the sensitivity of H2122AR30 cells to sotorasib. Overexpression of PTPRR indeed increased the sotorasib sensitivity of these cells compared with that apparent in control H2122AR30 cells expressing GFP, with IC_{50} values of 0.64 and 27.0 $\mu\text{mol/L}$, respectively (Fig. 3C).

We also investigated whether EGFR inhibition might affect intracellular signaling and restore sensitivity to sotorasib in H2122AR30 cells. Neither sotorasib nor the anti-EGFR antibody cetuximab alone had a substantial effect on the phosphorylation of ERK in H2122AR30 cells. Treatment with cetuximab alone resulted in partial inhibition of AKT phosphorylation, whereas sotorasib alone had no such effect. However, the combination of sotorasib and cetuximab attenuated the phosphorylation of both ERK and AKT (Fig. 3D). A cell viability assay also showed that cetuximab restored the anticancer effect of sotorasib in H2122AR30 cells (Supplementary Fig. S4A and S4B). We also performed a colony formation assay with H2122AR30 cells to evaluate the long-term efficacy of cetuximab. Colony formation by parental H2122 cells was suppressed by sotorasib alone, whereas that by H2122AR30 cells was not affected by sotorasib or cetuximab alone. Importantly, colony formation by H2122AR30 cells was abolished by exposure to the combination of sotorasib and cetuximab (Fig. 3E). Consistent with these findings, the combination of sotorasib and cetuximab also effectively overcame sotorasib resistance in PTPRR-downregulated SW837 cells, further supporting the role of EGFR signaling in mediating resistance downstream of PTPRR (Supplementary Fig. S5A and S5B). These results suggested that cetuximab was able to restore sensitivity to sotorasib by blocking EGFR-ERK signaling in PTPRR-deficient KRAS^{G12C}-mutant NSCLC cells.

PTPRR expression is regulated by promoter DNA methylation

PTPRR exists as two major variants in which expression is regulated by distinct promoters containing CpG islands (Fig. 4A; refs. 28–30). We found that the abundance of the mRNA for the short isoform of PTPRR was greater than that for the long form in NSCLC tumors of individuals in the dbGaP database (EAGLE study), with median values of 0.14 versus 0 ($n = 73$, $P < 0.001$); the short and long isoform mRNAs were detected in 76.7% (56 of 73) and 8.2% (6 of 73) of the tumor specimens (Fig. 4B). We then evaluated the relation between *PTPRR* expression and promoter methylation status in our H2122 cell lines as well as in SW1573, a KRAS^{G12C}-mutant NSCLC cell line that is resistant to sotorasib. Transcripts encoding the long isoform of PTPRR were not detected in any of these cell lines by RT-qPCR analysis. The mRNA for the short form of PTPRR was also essentially undetectable in SW1573 cells (Fig. 4C). The extent of CpG methylation in the promoter region for the short variant of PTPRR, as determined by bisulfite sequencing, was greatly increased in H2122AR14, H2122AR30, and SW1573 cells compared with H2122 cells (Fig. 4D), and it was inversely related to the abundance of the short-form mRNA in these cells (Fig. 4C and D). These results suggested that promoter methylation is responsible for the downregulation of *PTPRR* expression in the sotorasib-resistant cells.

EGFR blockade restores sensitivity to sotorasib in PTPRR-downregulated tumors *in vivo*

To determine whether EGFR inhibition might restore sensitivity to sotorasib in PTPRR-downregulated cancer *in vivo*, we evaluated the anticancer effect of the combination of sotorasib and cetuximab in cell line-derived xenograft (CDX) models with H2122 and H2122AR30 cells. Consistent with our *in vitro* observations, sotorasib markedly attenuated the growth of H2122 cell xenografts in nude mice, with this effect persisting for at least 28 days (Fig. 5A). In contrast, neither sotorasib nor cetuximab alone suppressed the growth of H2122AR30 xenograft tumors (Fig. 5B). However, the administration of both drugs prevented the growth of these tumors for at least 4 weeks (Fig. 5B; Supplementary Fig. S6A and S6B). Toxicity, including body weight loss, was not greater for the combination treatment than for either type of monotherapy (Fig. 5C and D). These results thus suggested that the resistance to sotorasib conferred by downregulation of PTPRR in KRAS^{G12C}-positive NSCLC can be overcome by combination therapy with sotorasib and cetuximab.

Impact of PTPRR expression on clinical outcome in patients with NSCLC treated with sotorasib

Given the role of PTPRR downregulation in resistance to KRAS^{G12C} inhibitors identified here in cell line models, we investigated the clinical relevance of PTPRR using human tumor specimens. RT-qPCR analysis revealed that the amount of PTPRR mRNA (short form) was significantly higher in NSCLC tumors ($n = 10$) than in normal lung tissue ($n = 9$) for the study cohort (median of 1.92 vs. 0, $P = 0.03$; Fig. 6A). Conversely, the DNA methylation level of the PTPRR promoter region (short form) was significantly lower in NSCLC tumor specimens than in normal lung tissue (median of 43 vs. 47, $P = 0.04$; Supplementary Fig. S7A). We also examined the methylation of the PTPRR promoter region (short form) for normal lung tissue ($n = 68$), peritumoral tissue ($n = 65$), and tumor tissue ($n = 146$) from patients with NSCLC in the dbGaP database. The methylation levels were found to be reduced in peritumoral (0.58 vs. 0.65, $P = 0.01$) and tumor (0.54 vs. 0.65, $P < 0.001$) tissue compared with normal tissue (Supplementary Fig. S7B). For a subset of cases with both RNA sequencing and methylation data available ($n = 10$), a trend toward a negative correlation between the abundance of PTPRR mRNA (short form) and the methylation of the PTPRR promoter region (short form) was apparent (Supplementary Fig. S7C).

We next examined the relationship between PTPRR expression and the clinical outcome of sotorasib treatment for 13 individuals with KRAS^{G12C}-mutant NSCLC in the current study cohort. The expression of PTPRR in the cytoplasm of tumor cells was evaluated by IHC staining (Fig. 6B). Patient characteristics are summarized in Supplementary Table S5. Of the 13 pretreatment tumor specimens, 8 and 5 showed high and low PTPRR expression, respectively, with none of the specimens being negative for PTPRR expression. Patients with low PTPRR expression tended to have a shorter PFS on sotorasib treatment [median of 4.3 months (95% CI, 2.4 months to not reached) vs. 7.5 months (95% CI, 1.6–12.5 months), log-rank test $P = 0.10$; HR of 3.27, with a 95% CI of 0.76–14; Fig. 6C] and a shorter OS [median of 7.5 months (95% CI, 5.4 months to not reached) vs. not reached (95% CI, 4.6 months to not reached), log-rank test $P = 0.13$; HR of 3.21, with a 95% CI of 0.70–14.7; Fig. 6D] than those with high PTPRR expression. These observations thus suggested that a low level of PTPRR expression in

tumor cells before treatment is associated with a poor clinical outcome of sotorasib treatment in patients with KRAS^{G12C}-mutant NSCLC.

Impact of PTPRR expression on clinical outcome in patients with NSCLC treated with EGFR tyrosine kinase inhibitors

Our *in vitro* data showed that PTPRR knockdown increased EGFR phosphorylation (Fig. 2H) as well as increased sensitivity to the EGFR tyrosine kinase inhibitor (TKI) osimertinib (Supplementary Fig. S8) in H1975 EGFR mutation-positive NSCLC cells, suggesting that PTPRR expression may also be associated with the therapeutic efficacy of EGFR-TKIs. We therefore evaluated the relationship between the abundance of PTPRR mRNA (short form) in pretreatment tumor specimens and the therapeutic efficacy of EGFR-TKIs in patients with EGFR-mutated NSCLC ($n = 17$). The characteristics of these patients are summarized in Supplementary Table S6. Individuals who acquired a secondary T790M mutation of EGFR were excluded because they tend to have a longer PFS than those without this mutation (31, 32). The amount of PTPRR mRNA in tumor specimens was determined by RNA-sequencing analysis (33). Patients with detectable PTPRR expression showed a significantly shorter PFS on EGFR-TKI treatment than those without such expression [median of 3 months (95% CI, 1.8 months to not reached) vs. 12.2 months (95% CI, 6.5–22.2 months), log-rank test $P < 0.001$; HR, not estimable; Supplementary Fig. S9]. Together, our preclinical and clinical observations suggested that EGFR activating mutation-positive NSCLC with downregulation of PTPRR may have a more favorable clinical outcome of EGFR-TKI treatment because such tumors are more dependent on EGFR signaling than those without PTPRR downregulation.

Discussion

We have shown that downregulation of PTPRR conferred resistance to the KRAS^{G12C} inhibitor sotorasib in KRAS^{G12C}-mutant NSCLC. Downregulation of PTPRR resulted in increased phosphorylation of EGFR on tyrosine residues, including Y1173 and consequent activation of the ERK signaling pathway. Expression of PTPRR seemed to be regulated by DNA methylation of the promoter region, with increased promoter methylation leading to sustained downregulation of PTPRR and constitutive activation of EGFR in sotorasib-resistant cells. Concomitant EGFR inhibition restored sensitivity to sotorasib in PTPRR-deficient cells, suggesting that the dual blockade of KRAS^{G12C} and EGFR is a rational therapeutic strategy for KRAS^{G12C}-mutant tumors with reduced expression of PTPRR.

We and others previously showed that MET amplification gives rise to sotorasib resistance in NSCLC (20, 27). Such MET activation promotes ERK signaling independently of KRAS^{G12C} (20, 27), a situation similar to the present finding of EGFR-dependent resistance to sotorasib. However, although MET amplification does not seem to occur frequently in KRAS^{G12C}-mutant cancers (20, 34), EGFR is frequently overexpressed in cancers, including NSCLC and colorectal cancer (35, 36). Of note, H2122 cells harbor not only KRAS^{G12C} but also KEAP1 and STK11 mutations, whereas SW1573 cells harbor KRAS^{G12C} together with the K111E mutation of PIK3CA. These mutations have been associated with a reduced sensitivity to KRAS^{G12C} inhibitors and may influence the dependence of these cells on EGFR (17, 37). In the present study, we found that EGFR activation was induced by downregulation of PTPRR in sotorasib-resistant cells. Consistent

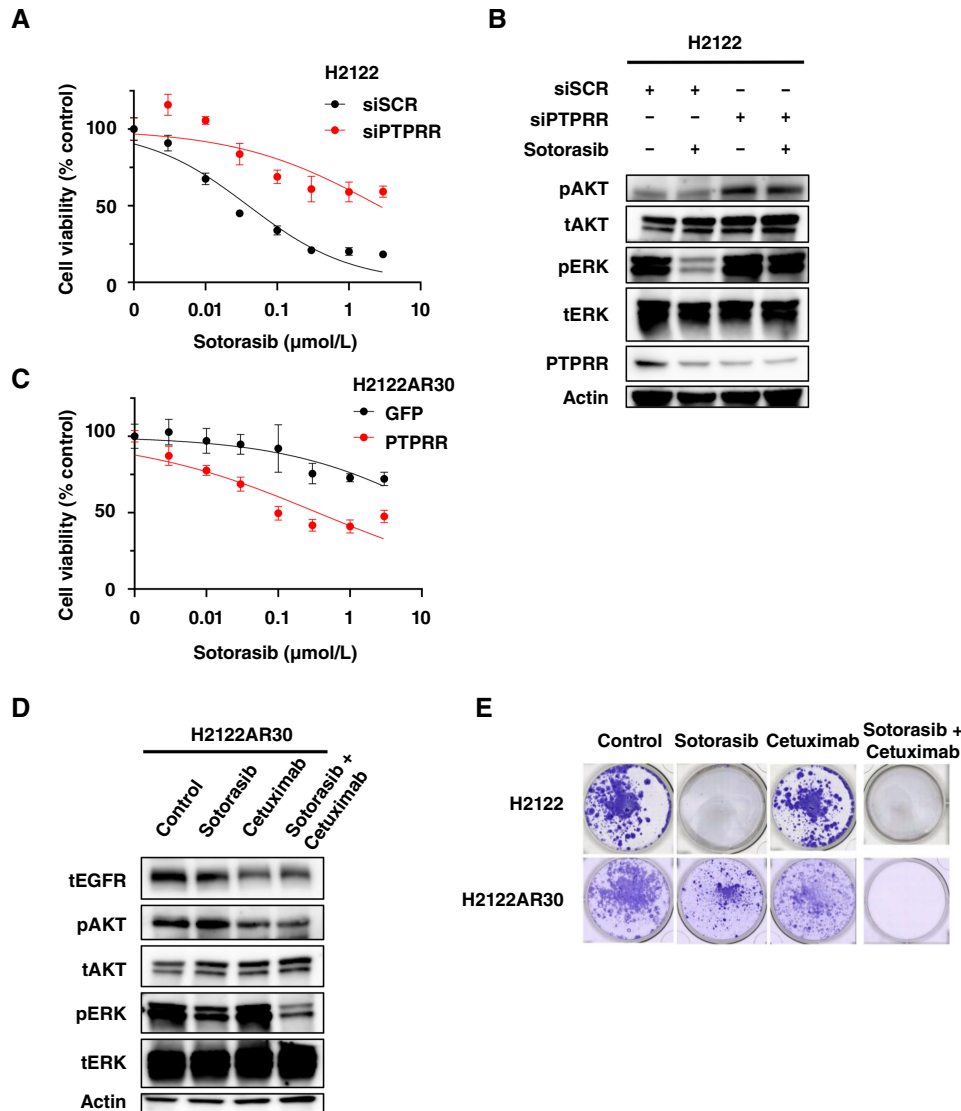


FIGURE 3. Combination treatment with EGFR and KRAS^{G12C} inhibitors overcomes sotorasib resistance due to PTPRR downregulation. **A**, Cell viability assay for H2122 cells transfected with nonspecific control (siSCR) or PTPRR-specific (siPTPRR) siRNAs and then exposed to the indicated concentrations of sotorasib for 72 hours. **B**, Immunoblot analysis of PTPRR as well as total and phosphorylated forms of AKT and ERK in H2122 cells transfected with siRNAs as in **(A)** and then incubated with or without sotorasib (1 $\mu\text{mol/L}$) for 4 hours. **C**, Cell viability assay for H2122AR30 cells stably transfected with control (GFP) or PTPRR expression plasmids and treated with the indicated concentrations of sotorasib for 72 hours. **D**, Immunoblot analysis of total or phosphorylated forms of EGFR, AKT, and ERK in H2122AR30 cells treated with sotorasib (1 $\mu\text{mol/L}$), cetuximab (10 $\mu\text{g/mL}$), or the combination of both drugs for 4 hours. **E**, Colony formation assay for H2122 and H2122AR30 cells incubated with or without sotorasib (1 $\mu\text{mol/L}$), cetuximab (10 $\mu\text{g/mL}$), or both drugs for 4 weeks. Surviving cells were stained with crystal violet. Data in **A** and **C** are means \pm SD ($n = 3$ independent experiments), and those in **B**, **D**, and **E** are representative of at least three independent experiments.

with this finding, EGFR-driven reactivation of MAPK/ERK signaling has previously been identified as a dominant mechanism of primary resistance to KRAS^{G12C} inhibition (18, 36). Furthermore, dual blockade of EGFR and KRAS^{G12C} signaling was previously found to be more effective than treatment with an EGFR inhibitor or KRAS^{G12C} inhibitor alone in some cancer cells harboring the KRAS^{G12C} mutation (15, 38, 39). Combined inhibition of EGFR and KRAS^{G12C} was also shown to have synergistic antitumor effects in NSCLC models (40, 41). Although various combination therapies, including a KRAS^{G12C} inhibitor, have been developed clinically, combinations with an

EGFR inhibitor have shown efficacy in refractory cancers. A phase II trial (KROCUS) that evaluated the safety and efficacy of combination therapy with the KRAS^{G12C} inhibitor fulzerasib and cetuximab for treatment-naïve KRAS^{G12C}-mutant NSCLC demonstrated a high response rate of 81.8% and a disease control rate of 100% (42). In addition, a phase Ib trial that assessed the combination of sotorasib and the anti-EGFR antibody panitumumab in individuals with previously treated KRAS^{G12C}-mutant NSCLC reported a response rate of 47.5% (43). Sotorasib and adagrasib have also been approved by the FDA for combination therapy together with an EGFR inhibitor

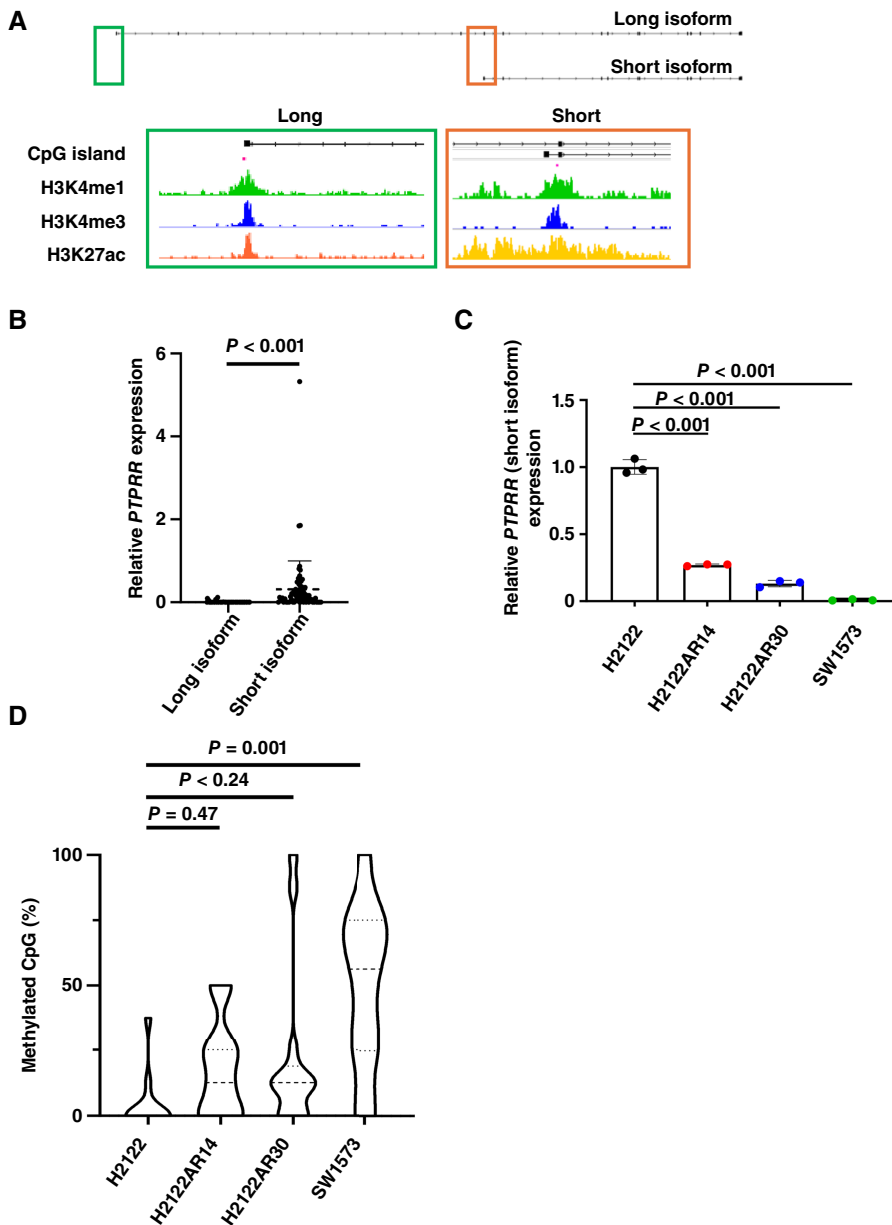


FIGURE 4. Expression of *PTPRR* is regulated by promoter DNA methylation in *KRAS*^{G12C}-mutant NSCLC cell lines. **A**, The human *PTPRR* gene including the promoter regions for the long and short isoforms of the encoded protein is shown. The positions of CpG islands as well as the histone marks H3K4me1, H3K4me3, and H3K27ac are indicated. **B**, Abundance of transcripts for the long and short isoforms of *PTPRR* in tumor specimens from patients with NSCLC in the dbGaP database ($n = 73$). Data are presented as dot plots with means \pm SD indicated by the dashed and solid lines for the short isoform, and they were analyzed with the Wilcoxon ranked-sum test. **C**, RT-qPCR analysis of mRNA abundance for the short form of *PTPRR* in the indicated *KRAS*^{G12C}-mutant cell lines. Data are presented as dot plots, with means \pm SD being indicated by the dashed and solid lines ($n = 3$ independent experiments) and analyzed by one-way ANOVA and Dunnett's test. **D**, Bisulfite genomic sequencing of the promoter region for the short variant of *PTPRR* in the indicated *KRAS*^{G12C}-mutant cell lines. The percentage of methylated CpG sites among total CpG sites is shown. Data are presented as violin plots, with the median and upper quartile values indicated by the dashed and dotted lines and analyzed by one-way ANOVA and Dunnett's test. Data are representative of three independent experiments.

(panitumumab or cetuximab) for *KRAS*^{G12C}-mutant colorectal cancer (15, 38, 39). Activation of EGFR by downregulation of *PTPRR* may underlie the efficacy of combined treatment with EGFR and *KRAS* inhibitors. Our preliminary examination of clinical specimens suggested that low *PTPRR* expression was associated with a poor clinical outcome in patients with NSCLC treated with the *KRAS*^{G12C} inhibitor sotorasib. The results obtained with our CDX models also indicated that the combination of an anti-EGFR antibody and *KRAS*^{G12C} inhibitor may be more effective than either monotherapy for *PTPRR*-deficient tumors.

Our study suggests that *PTPRR* plays a key role in the regulation of EGFR-ERK signaling in *KRAS*^{G12C}-mutant cancer as well as in *EGFR* mutation-positive cancer. The extent of protein tyrosine phosphorylation is determined dynamically by the balance between the activities of protein tyrosine kinases and PTPs (44–46). The loss of PTPs, which can result from genetic

alterations or epigenetic changes such as promoter DNA methylation (as in the case of *PTPRR*), has been shown to lead to the hyperactivation of signaling pathways (46). *PTPRR* has been identified as a physiologic regulator of ERK signaling in several cancer types (28, 47, 48). *PTPRR* interacts with multiple RTKs (49), but little has been known about its association with EGFR. Our results now suggest that *PTPRR* inhibits EGFR signaling by associating with EGFR and mediating its dephosphorylation and that *PTPRR* expression is regulated by promoter methylation. DNA methylation is an important mechanism of gene silencing and plays a pivotal role in cancer development. Inhibition of the MAPK pathway has been shown to disturb DNA methylation (50, 51). We speculate that inhibition of ERK signaling by sotorasib may therefore have disrupted DNA methylation and resulted in downregulation of *PTPRR* expression although such a mechanism was not directly demonstrated in the present study. Phosphorylation of EGFR on tyrosine residues, most prominently at Y1173, was increased in

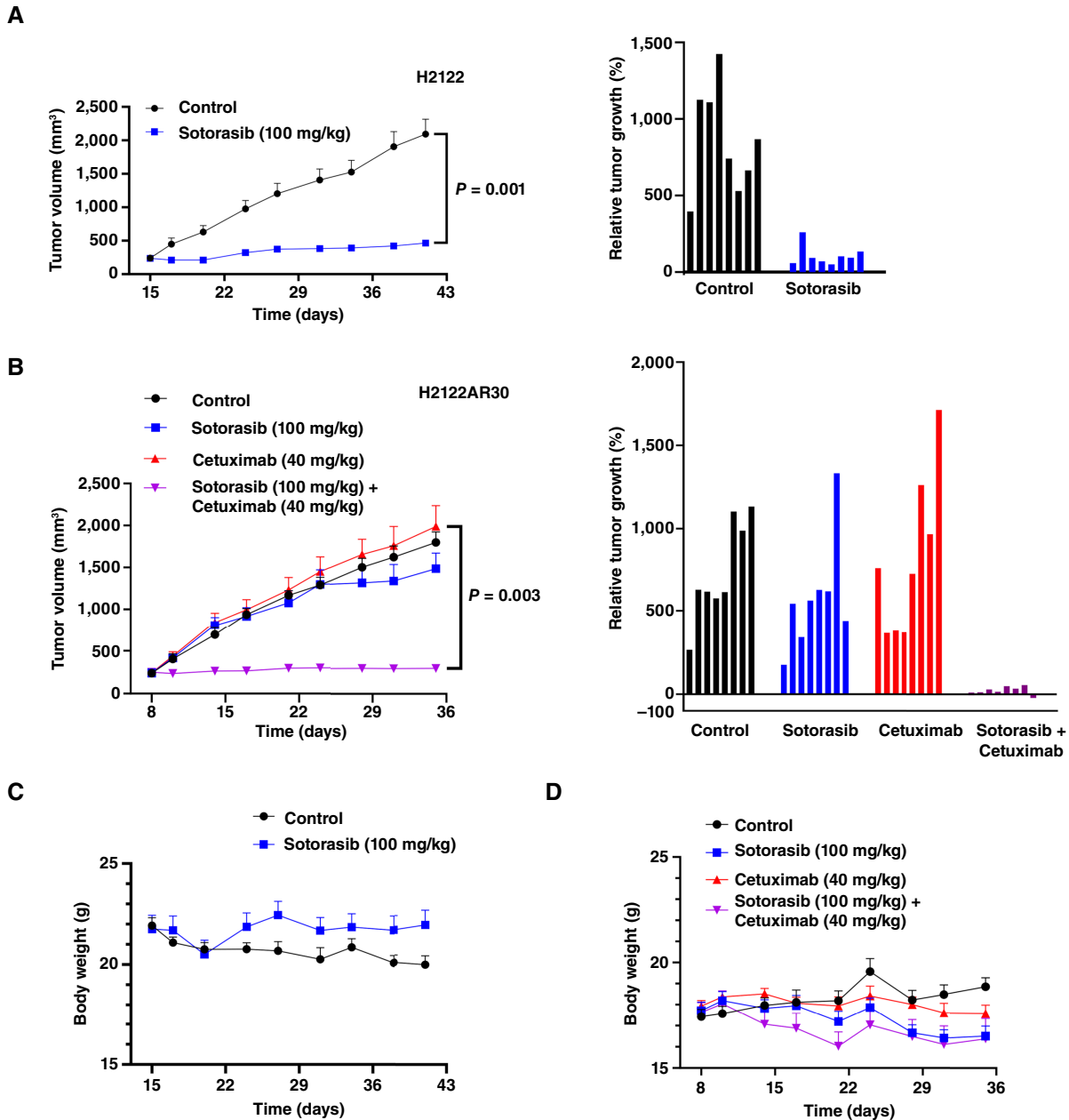


FIGURE 5. EGFR inhibition overcomes resistance to sotorasib in CDX tumors. Experiments were performed using H2122 (**A**) and PTPRR-downregulated H2122AR30 cells (**B**). **A**, Nude mice harboring H2122 xenografts were treated orally with sotorasib (100 mg/kg, daily) or vehicle (control). The time course of mean tumor volume (left) and relative tumor growth for individual tumors ($n = 8$) after treatment for 28 days (right) is shown. **B**, Nude mice harboring H2122AR30 xenografts were treated orally with sotorasib (100 mg/kg, daily) and i.p. with cetuximab (40 mg/kg, twice weekly) as indicated. The time course of mean tumor volume (left) and relative tumor growth for individual tumors ($n = 8$) after treatment for 28 days (right) is shown. **C** and **D**, Time course of mean body weight for tumor-bearing mice as in **A** and **B**, respectively. All time course data are means \pm SEM. The P values for the indicated comparisons in **A** and **B** were determined using the unpaired t test.

PTPRR-deficient cells; however, it remains unclear which tyrosine residues are directly targeted by PTPRR. Although phosphorylation at Y1173 was most pronounced, additional EGFR phosphorylation sites not assessed in the present study may play a role in the regulation of downstream ERK signaling, as previously described (52). Y1173 is the most COOH-terminal phosphorylation site of EGFR and activates downstream signaling through

binding to the adapter protein SHC (53, 54). Knockout of PTPRH, another member of the PTP family, was recently shown to result in a selective increase in EGFR phosphorylation at Y1173 (bioRxiv 2024.06.13.598886), suggesting that individual PTP family members may differentially regulate phosphorylation at specific EGFR tyrosine residues. PTPRR may similarly influence EGFR phosphorylation in a site-specific manner. In addition to PTPRR, mitogen-induced

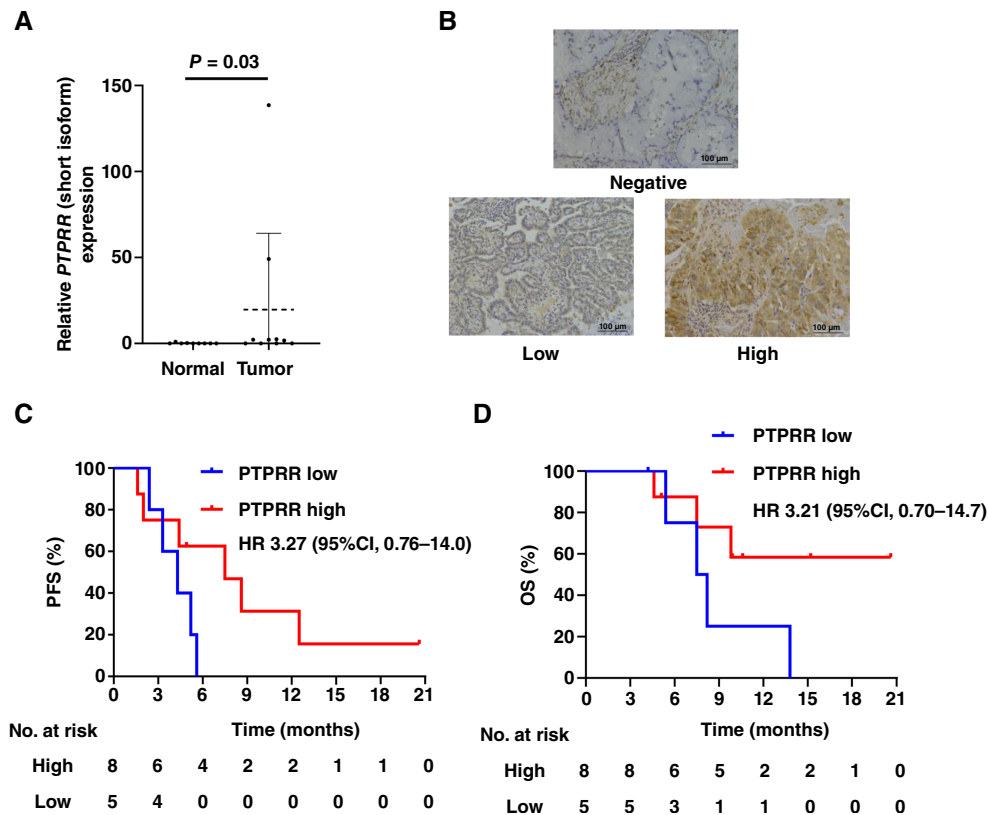


FIGURE 6. Clinical relevance of PTPRR expression to sotorasib treatment in individuals with NSCLC. **A**, RT-qPCR analysis of PTPRR mRNA (short form) abundance in normal lung tissue ($n = 9$) and NSCLC tumor tissue ($n = 10$). Data are presented as dot plots with means \pm SD indicated by the dashed and solid lines, and they were analyzed with the Wilcoxon ranked-sum test. **B**, Representative IHC images for specimens of normal lung tissue (negative) and NSCLC tumor tissue (low and high) stained with antibodies to PTPRR. Scale bars, 100 μ m. **C** and **D**, Kaplan-Meier analysis of PFS (**C**) and OS (**D**) according to low ($n = 5$) or high ($n = 8$) status for cytoplasmic PTPRR staining in tumor cells for patients with KRAS^{G12C}-mutant NSCLC treated with sotorasib.

gene 6 (MIG6, encoded by *ERRF1*) has been identified as a negative regulator of EGFR, and its downregulation has been associated with resistance to ALK/ROS1 inhibitors mediated by EGFR-dependent signaling (55). Our microarray analysis did not reveal downregulation of *ERRF1* expression in sotorasib-resistant cells. However, given that we did not examine MIG6 protein levels, we cannot conclude that the observed increase in EGFR phosphorylation is attributable solely to reduced PTPRR expression.

Our study has some limitations. First, the number of clinical specimens examined was small, and the results obtained with these specimens remain to be validated. Given the heterogeneity of tumors, larger-scale studies are warranted to clarify the relation between PTPRR expression and sotorasib efficacy in individuals with KRAS^{G12C}-mutant NSCLC. The trends observed with clinical specimens from individuals with KRAS^{G12C}-mutant and EGFR-mutant NSCLC did not achieve statistical significance and should, therefore, be interpreted as hypothesis-generating observations rather than as definitive conclusions. Second, the study did not evaluate changes in PTPRR expression before and after sotorasib treatment with paired pre- and posttreatment specimens, with future investigations needed to address this limitation. Third, mutations in the genes for other receptor-type PTPs—including PTPRT, PTPRD, and PTPRM—have been identified in various cancer types (56). Whether these genetic alterations influence EGFR dependency or interact with PTPRR downregulation warrants further investigation.

Data Availability

The data generated in this study are included in the main article and Supplementary information. Raw data are available on request without

restriction from the corresponding author. Other data have been uploaded to NCBI Gene Expression Omnibus (<https://www.ncbi.nlm.nih.gov/geo/>) under data repository accession number GSE295133 and NCBI Sequence Read Archive (<https://www.ncbi.nlm.nih.gov/sra>) database under data repository BioProject accession number PRJNA1262108. Source data are provided with this article. Additional methods are included in Supplementary Methods.

Authors' Disclosures

H. Kanemura reports grants from the Japan Society for the Promotion of Science during the conduct of the study as well as grants from Chugai Pharmaceutical Co. Ltd. and Takeda Pharmaceutical Co. Ltd. and personal fees from Chugai Pharmaceutical Co. Ltd., AstraZeneca K.K., Daiichi Sankyo Co. Ltd., and Novartis Pharma K.K. outside the submitted work. S. Tomida reports grants from Illumina Inc. outside the submitted work. K. Kunimasa reports grants from Ono Pharmaceutical Co. Ltd., Taiho Pharmaceutical Co. Ltd., Eli Lilly Japan, AbbVie, Daiichi Sankyo Co. Ltd., Amgen, Eisai Co. Ltd., Sanofi K.K., Janssen Pharmaceutical K.K., Novartis Pharmaceuticals, Pfizer, Merck Biopharma Co. Ltd., Takeda Pharmaceutical Co. Ltd., AstraZeneca, Merus NV, MSD, Bayer Yakuin Ltd., Delta-Fly Pharma Inc., IQVIA Holdings Inc., Nippon Boehringer Ingelheim Co. Ltd., and Parexel International Inc. and personal fees from Amgen, AstraZeneca, Daiichi Sankyo Co. Ltd., Eli Lilly Japan, Janssen Pharmaceutical K.K., Merck Biopharma Co. Ltd., MSD, Novartis Pharmaceuticals, Ono Pharmaceutical Co. Ltd., and Pfizer outside the submitted work. T. Nakayama reports personal fees from Daiichi Sankyo Co. Ltd., MSD K.K., Kyowa Kirin Co. Ltd., Hisamitsu Pharmaceutical Co. Inc., Eli Lilly Japan K.K., Chugai Pharmaceutical Co. Ltd., and Taiho Pharmaceutical Co. Ltd. outside the submitted work.

S. Watanabe reports personal fees from Daiichi Sankyo Co. Ltd., Chugai Pharmaceutical Co. Ltd., MSD K.K., Eli Lilly Japan K.K., Kyowa Kirin Co. Ltd., and Eisai Co. Ltd. outside the submitted work. S. Suzuki reports grants from Boehringer Ingelheim and Japan Boehringer Ingelheim outside the submitted work. K. Sakai reports personal fees from Takeda Pharmaceutical Co. Ltd., Nippon Kayaku Co. Ltd., QIAGEN Inc., and Life Technologies Japan Ltd. outside the submitted work. K. Azuma reports grants and personal fees from AstraZeneca, MSD, Chugai Pharmaceutical, Bristol Myers Squibb, Taiho Pharmaceutical, and AMGEN; personal fees from Ono Pharmaceutical and Takeda Pharmaceutical; and grants from Janssen Pharmaceutical, Daiichi Sankyo, IQVIA, EPS, and Syneos outside the submitted work. K. Nishio reports grants and personal fees from Eli Lilly Japan and Otsuka Pharmaceutical, grants from Thoracic Oncology Research Group; grants from Hitachi, Okayama University, Nippon Boehringer Ingelheim, West Japan Oncology Group, Japan Breast Cancer Research Group, and Kyushu Study Group of Clinical Cancer; and personal fees from AstraZeneca, Guardant Health, Janssen Pharmaceutical, Daiichi Sankyo, Nichirei, Maruho, Osakaminami Hospital, Nittobo Medical, Nihon Servier, Symbio Pharmaceuticals, Chugai, and MSD outside the submitted work. K. Nakagawa reports grants from IQVIA Services Japan K.K., Syneos Health Clinical K.K., EPS Corporation, Nippon Kayaku Co. Ltd., Takeda Pharmaceutical Co. Ltd., MSD K.K., Amgen Inc., Taiho Pharmaceutical Co. Ltd., Bristol Myers Squibb, Janssen Pharmaceutical K.K., CMIC Co. Ltd., Pfizer R&D Japan G.K., Labcorp Development Japan K.K., Kobayashi Pharmaceutical Co. Ltd., Pfizer Japan Inc., AbbVie Inc., Japan Clinical Cancer Research Organization, Eisai Co. Ltd., EP-CRSU Co. Ltd., Shionogi & Co. Ltd., Otsuka Pharmaceutical Co. Ltd., GlaxoSmithKline K.K., Sanofi K.K., Chugai Pharmaceutical Co. Ltd., Nippon Boehringer Ingelheim Co. Ltd., SRL Medisearch Inc., PRA Health Sciences Inc., Astellas Pharma Inc., Ascent Development Services, Eisai Inc., Bayer Yakuhin Ltd., AstraZeneca K.K., A2 Healthcare Corp., Thoracic Oncology Research Group, Ono Pharmaceutical Co. Ltd., Eli Lilly Japan K.K., Daiichi Sankyo Co. Ltd., AstraZeneca K.K., Chugai Pharmaceutical Co. Ltd., MSD K.K., Pfizer Japan Inc., Nippon Boehringer Ingelheim Co. Ltd., Incyte Biosciences Japan, Otsuka Pharmaceutical Factory Inc., Hisamitsu Pharmaceutical Co. Inc., Patientricity MedPartners K.K., Merck Biopharma Co. Ltd., Bayer Yakuhin Ltd., Novartis Pharma K.K., Bristol Myers Squibb Company, Janssen Pharmaceutical K.K., Taiho Pharmaceutical Co. Ltd., Medical Mobile Communications Co., Ltd., Yodosha Co. Ltd., M3 Inc., Global Health Consulting Japan Co. Ltd., The Yomiuri Shimbun, and 3H Medi Solution Inc. outside the submitted work. H. Hayashi reports personal fees from Bristol Myers Squibb K.K., Chugai Pharmaceutical Co. Ltd., Eli Lilly Japan K.K., Ono Pharmaceutical Co. Ltd., MSD K.K., AstraZeneca K.K., Janssen Pharmaceutical K.K., Amgen K.K., Taiho Pharmaceutical Co. Ltd., AbbVie GK, Japan Board of Cancer Therapy, Kyowa Kirin Co. Ltd., Daiichi Sankyo Co. Ltd., Pfizer Japan Inc., Japanese Society of Medical Oncology, Novocure K.K., Nippon Kayaku Co. Ltd., Nippon Boehringer Ingelheim Co. Ltd., Nikkei Video Productions Inc., The Japanese Society of Internal Medicine, Regeneron Pharmaceuticals Inc., CMIC Inizio Co. Ltd., BeiGene Medicines GK, Exact Sciences Corp., Ministry of Health, Labour and Welfare and grants from IQVIA Services Japan K.K., Eisai Co. Ltd., Syneos Health Clinical K.K., EP-CRSU Co., Ltd., EPS Corporation, Shionogi & Co. Ltd., Nippon Kayaku Co. Ltd., Otsuka Pharmaceutical Co. Ltd., Takeda Pharmaceutical Co. Ltd., GlaxoSmithKline K.K., MSD K.K., Sanofi K.K., Amgen Inc., Chugai Pharmaceutical Co. Ltd., Taiho Pharmaceutical Co. Ltd., Nippon Boehringer Ingelheim Co. Ltd., Bristol

Myers Squibb Company, SRL Medisearch Inc., Janssen Pharmaceutical K.K., PRA Health Sciences Inc., CMIC Co., Ltd., Astellas Pharma Inc., Pfizer R&D Japan G.K., Ascent Development Services, Labcorp Development Japan K.K., Eisai Inc., Kobayashi Pharmaceutical Co. Ltd., Bayer Yakuhin, Ltd., Pfizer Japan Inc., AstraZeneca K.K., AbbVie Inc., Daiichi Sankyo Co. Ltd., A2 Healthcare Corp., Novartis Pharma K.K., Eli Lilly Japan K.K., Merck Biopharma Co. Ltd., Medpace Japan K.K., Kyowa Kirin Co. Ltd., PPD-SNBL K.K., ICON Japan K.K., Mochida Pharmaceutical Co. Ltd., Sysmex Corporation, Clinical Research Support Center Kyushu, Kyushu Study Group of Clinical Cancer, Public Health Research Foundation, Thoracic Oncology Research Group, Japanese Gastric Cancer Association, West Japan Oncology Group, Aichi Cancer Network, Osaka Gyoumeikan Hospital, Japan Clinical Cancer Research Organization, and Comprehensive Support Project for Oncological Research of Breast Cancer outside the submitted work. K. Yonesaka reports grants from Daiichi Sankyo Co. Ltd. and personal fees from Daiichi Sankyo Co. Ltd. and AstraZeneca K.K. outside the submitted work and a patent to Daiichi Sankyo Co. Ltd. pending. No disclosures were reported by the other authors.

Authors' Contributions

H. Kanemura: Conceptualization, resources, data curation, formal analysis, funding acquisition, validation, investigation, methodology, writing—original draft, writing—review and editing. **T. Takehara:** Conceptualization, data curation, formal analysis, validation, investigation, methodology, writing—original draft, writing—review and editing. **O. Maenishi:** Investigation, methodology. **S. Tomida:** Conceptualization, software, formal analysis, methodology, writing—review and editing. **N. Iwakaki:** Data curation, validation, investigation, methodology. **K. Kunimasa:** Resources, data curation. **T. Nakayama:** Resources, data curation. **S. Watanabe:** Resources, data curation. **S. Suzuki:** Investigation, methodology. **K. Sakai:** Investigation, methodology. **K. Azuma:** Resources, data curation. **K. Kudo:** Resources, data curation. **K. Nishio:** Investigation, methodology. **K. Nakagawa:** Supervision, funding acquisition, project administration. **H. Hayashi:** Supervision, funding acquisition, project administration. **T. Teramura:** Conceptualization, supervision, investigation, methodology, writing—original draft, project administration, writing—review and editing. **K. Yonesaka:** Conceptualization, supervision, funding acquisition, investigation, methodology, writing—original draft, project administration, writing—review and editing.

Acknowledgments

We thank Haruka Sakamoto, Michiko Kitano, and Yume Shinkai at the Department of Medical Oncology, Kindai University Faculty of Medicine, for their technical support. This work was supported by Grants-in-Aid for Scientific Research (21K07204 to K. Yonesaka and 24K18560 to H. Kanemura) from the Japan Society for the Promotion of Science.

Note

Supplementary data for this article are available at Cancer Research Communications Online (<https://aacrjournals.org/cancerrescommun/>).

Received August 24, 2025; revised January 30, 2026; accepted March 09, 2026; posted first April 02, 2026.

References

- Simanshu DK, Nissley DV, McCormick F. RAS proteins and their regulators in human disease. *Cell* 2017;170:17–33.
- Ostrem JM, Peters U, Sos ML, Wells JA, Shokat KM. K-Ras(G12C) inhibitors allosterically control GTP affinity and effector interactions. *Nature* 2013;503:548–51.
- Moore AR, Rosenberg SC, McCormick F, Malek S. RAS-targeted therapies: is the undruggable druggable? *Nat Rev Drug Discov* 2020;19:533–52.
- Singhal A, Li BT, O'Reilly EM. Targeting KRAS in cancer. *Nat Med* 2024;30:969–83.
- Prior IA, Hood FE, Hartley JL. The frequency of Ras mutations in cancer. *Cancer Res* 2020;80:2969–74.
- Nassar AH, Adib E, Kwiatkowski DJ. Distribution of KRAS^{G12C} somatic mutations across race, sex, and cancer type. *N Engl J Med* 2021;384:185–7.
- Canon J, Rex K, Saiki AY, Mohr C, Cooke K, Bagal D, et al. The clinical KRAS(G12C) inhibitor AMG 510 drives anti-tumour immunity. *Nature* 2019;575:217–23.
- Skoulidis F, Li BT, Dy GK, Price TJ, Falchook GS, Wolf J, et al. Sotorasib for lung cancers with KRAS p.G12C mutation. *N Engl J Med* 2021;384:2371–81.
- Jänne PA, Riely GJ, Gadgeel SM, Heist RS, Ou S-HI, Pacheco JM, et al. Adagrasib in non-small-cell lung cancer harboring a KRAS(G12C) mutation. *N Engl J Med* 2022;387:120–31.
- Lito P, Solomon M, Li L-S, Hansen R, Rosen N. Allele-specific inhibitors inactivate mutant KRAS G12C by a trapping mechanism. *Science* 2016;351:604–8.
- Soria J-C, Ohe Y, Vansteenkiste J, Reungwetwattana T, Chewaskulyong B, Lee KH, et al. Osimertinib in untreated EGFR-mutated advanced non-small-cell lung cancer. *N Engl J Med* 2018;378:113–25.
- Peters S, Camidge DR, Shaw AT, Gadgeel S, Ahn JS, Kim D-W, et al. Alectinib versus crizotinib in untreated ALK-positive non-small-cell lung cancer. *N Engl J Med* 2017;377:829–38.
- Mok T, Camidge DR, Gadgeel SM, Rosell R, Dziadziuszko R, Kim DW, et al. Updated overall survival and final progression-free survival data for patients with treatment-naive advanced ALK-positive non-small-cell lung cancer in the ALEX study. *Ann Oncol* 2020;31:1056–64.
- Fakhri MG, Kopetz S, Kuboki Y, Kim TW, Munster PN, Krauss JC, et al. Sotorasib for previously treated colorectal cancers with KRAS(G12C) mutation (Code-Break100): a prespecified analysis of a single-arm, phase 2 trial. *Lancet Oncol* 2022;23:115–24.
- Yaeger R, Weiss J, Pelster MS, Spira AI, Barve M, Ou S-I, et al. Adagrasib with or without cetuximab in colorectal cancer with mutated KRAS G12C. *N Engl J Med* 2023;388:44–54.
- Strickler JH, Satake H, George TJ, Yaeger R, Hollebecque A, Garrido-Laguna I, et al. Sotorasib in KRAS p.G12C-mutated advanced pancreatic cancer. *N Engl J Med* 2023;388:33–43.
- Negrao MV, Araujo HA, Lamberti G, Cooper AJ, Akhave NS, Zhou T, et al. Comutations and KRASG12C inhibitor efficacy in advanced NSCLC. *Cancer Discov* 2023;13:1556–71.
- Ryan MB, Fece de la Cruz F, Phat S, Myers DT, Wong E, Shahzade HA, et al. Vertical pathway inhibition overcomes adaptive feedback resistance to KRAS^{G12C} inhibition. *Clin Cancer Res* 2020;26:1633–43.
- Tanaka N, Lin JJ, Li C, Ryan MB, Zhang J, Kiedrowski LA, et al. Clinical acquired resistance to KRAS^{G12C} inhibition through a novel KRAS switch-II pocket mutation and polyclonal alterations converging on RAS-MAPK reactivation. *Cancer Discov* 2021;11:1913–22.
- Awad MM, Liu S, Rybkin II, Arbour KC, Dilly J, Zhu VW, et al. Acquired resistance to KRAS^{G12C} inhibition in cancer. *N Engl J Med* 2021;384:2382–93.
- Zhao Y, Murciano-Goroff YR, Xue JY, Ang A, Lucas J, Mai TT, et al. Diverse alterations associated with resistance to KRAS^{G12C} inhibition. *Nature* 2021;599:679–83.
- Tong X, Patel AS, Kim E, Li H, Chen Y, Li S, et al. Adeno-to-squamous transition drives resistance to KRAS inhibition in LKB1 mutant lung cancer. *Cancer Cell* 2024;42:413–28.e7.
- Perurena N, Situ L, Cichowski K. Combinatorial strategies to target RAS-driven cancers. *Nat Rev Cancer* 2024;24:316–37.
- Yonesaka K, Zejnullahu K, Okamoto I, Satoh T, Cappuzzo F, Souglakos J, et al. Activation of ERBB2 signaling causes resistance to the EGFR-directed therapeutic antibody cetuximab. *Sci Transl Med* 2011;3:99ra86.
- Xie T, Peng S, Liu S, Zheng M, Diao W, Ding M, et al. Multi-cohort validation of Ascove: an anokis-based prognostic signature for predicting disease progression and immunotherapy response in bladder cancer. *Mol Cancer* 2024;23:30.
- Kim MH, Kim YK, Shin DH, Lee HJ, Shin N, Kim A, et al. Yes associated protein is a poor prognostic factor in well-differentiated lung adenocarcinoma. *Int J Clin Exp Pathol* 2015;8:15933–9.
- Suzuki S, Yonesaka K, Teramura T, Takehara T, Kato R, Sakai H, et al. KRAS inhibitor resistance in MET-amplified KRAS^{G12C} non-small cell lung cancer induced by RAS- and non-RAS-mediated cell signaling mechanisms. *Clin Cancer Res* 2021;27:5697–707.
- Pulido R, Zúñiga A, Ullrich A. PTP-SL and STEP protein tyrosine phosphatases regulate the activation of the extracellular signal-regulated kinases ERK1 and ERK2 by association through a kinase interaction motif. *EMBO J* 1998;17:7337–50.
- Menigatti M, Cattaneo E, Sabates-Bellver J, Ilinsky VV, Went P, Buffoli F, et al. The protein tyrosine phosphatase receptor type R gene is an early and frequent target of silencing in human colorectal tumorigenesis. *Mol Cancer* 2009;8:124.
- Su PH, Lin YW, Huang RL, Liao YP, Lee HY, Wang HC, et al. Epigenetic silencing of PTPRR activates MAPK signaling, promotes metastasis and serves as a biomarker of invasive cervical cancer. *Oncogene* 2013;32:15–26.
- Wang S, Yan B, Zhang Y, Xu J, Qiao R, Dong Y, et al. Different characteristics and survival in non-small cell lung cancer patients with primary and acquired EGFR T790M mutation. *Int J Cancer* 2019;144:2880–6.
- Eide IJ, Helland Å, Ekman S, Mellemegaard A, Hansen KH, Cicas S, et al. Osimertinib in T790M-positive and -negative patients with EGFR-mutated advanced non-small cell lung cancer (the TREM-study). *Lung Cancer* 2020;143:27–35.
- Yonesaka K, Tanizaki J, Maenishi O, Haratani K, Kawakami H, Tanaka K, et al. HER3 augmentation via blockade of EGFR/AKT signaling enhances anticancer activity of HER3-targeting patritumab deruxtecan in EGFR-mutated non-small cell lung cancer. *Clin Cancer Res* 2022;28:390–403.
- Scheffler M, Ihle MA, Hein R, Merkelbach-Bruse S, Scheel AH, Siemanowski J, et al. K-ras mutation subtypes in NSCLC and associated co-occurring mutations in other oncogenic pathways. *J Thorac Oncol* 2019;14:606–16.
- Selvaggi G, Novello S, Torri V, Leonardo E, De Giuli P, Borasio P, et al. Epidermal growth factor receptor overexpression correlates with a poor prognosis in completely resected non-small-cell lung cancer. *Ann Oncol* 2004;15:28–32.
- Amodio V, Yaeger R, Arcella P, Cancelliere C, Lamba S, Lorenzato A, et al. EGFR blockade reverts resistance to KRAS^{G12C} inhibition in colorectal cancer. *Cancer Discov* 2020;10:1129–39.
- Skoulidis F, Li BT, de Langen AJ, Hong DS, Lena H, Wolf J, et al. Molecular determinants of sotorasib clinical efficacy in KRAS^{G12C}-mutated non-small-cell lung cancer. *Nat Med* 2025;31:2755–67.
- Yaeger R, Uboha NV, Pelster MS, Bekaii-Saab TS, Barve M, Saltzman J, et al. Efficacy and safety of adagrasib plus cetuximab in patients with KRASG12C-mutated metastatic colorectal cancer. *Cancer Discov* 2024;14:982–93.
- Fakhri MG, Salvatore L, Esaki T, Modest DP, Lopez-Bravo DP, Taieb J, et al. Sotorasib plus panitumumab in refractory colorectal cancer with mutated KRAS G12C. *N Engl J Med* 2023;389:2125–39.
- Patricelli MP, Janes MR, Li L-S, Hansen R, Peters U, Kessler LV, et al. Selective inhibition of oncogenic KRAS output with small molecules targeting the inactive state. *Cancer Discov* 2016;6:316–29.

41. Hallin J, Engstrom LD, Hargis L, Calinisan A, Aranda R, Briere DM, et al. The KRAS^{G12C} inhibitor MRTX849 provides insight toward therapeutic susceptibility of KRAS-mutant cancers in mouse models and patients. *Cancer Discov* 2020;10:54-71.
42. Gregorc V, González-Cao M, Salvagni S, Koumariou A, Gil-Bazo I, Maio M, et al. KROCUS: a phase II study investigating the efficacy and safety of fulzerasib (GFH925) in combination with cetuximab in patients with previously untreated advanced KRAS G12C mutated NSCLC. *J Clin Oncol* 2024;42(17_suppl):LBA8511.
43. Langer CJ, Galot R, Prenen H, Hong DS, Victoria I, Salgia R, et al. Sotorasib plus panitumumab for pre-treated non-small cell lung cancer with KRAS G12C mutation: a phase 1b study. *J Clin Oncol* 2024;42(16_suppl):8559.
44. Ostman A, Hellberg C, Böhmer FD. Protein-tyrosine phosphatases and cancer. *Nat Rev Cancer* 2006;6:307-20.
45. Tonks NK. Protein tyrosine phosphatases: from genes, to function, to disease. *Nat Rev Mol Cell Biol* 2006;7:833-46.
46. Bollu LR, Mazumdar A, Savage MI, Brown PH. Molecular pathways: targeting protein tyrosine phosphatases in cancer. *Clin Cancer Res* 2017;23:2136-42.
47. Buschbeck M, Eickhoff J, Sommer MN, Ullrich A. Phosphotyrosine-specific phosphatase PTP-SL regulates the ERK5 signaling pathway. *J Biol Chem* 2002;277:29503-9.
48. Munkley J, Lafferty NP, Kalna G, Robson CN, Leung HY, Rajan P, et al. Androgen-regulation of the protein tyrosine phosphatase PTPRR activates ERK1/2 signalling in prostate cancer cells. *BMC Cancer* 2015;15:9.
49. Yao Z, Darowski K, St-Denis N, Wong V, Offensperger F, Villedieu A, et al. A global analysis of the receptor tyrosine kinase-protein phosphatase interactome. *Mol Cell* 2017;65:347-60.
50. Lu R, Wang X, Chen ZF, Sun DF, Tian XQ, Fang JY. Inhibition of the extracellular signal-regulated kinase/mitogen-activated protein kinase pathway decreases DNA methylation in colon cancer cells. *J Biol Chem* 2007;282:12249-59.
51. Choi J, Huebner AJ, Clement K, Walsh RM, Savol A, Lin K, et al. Prolonged Mek1/2 suppression impairs the developmental potential of embryonic stem cells. *Nature* 2017;548:219-23.
52. Sordella R, Bell DW, Haber DA, Settleman J. Gefitinib-sensitizing EGFR mutations in lung cancer activate anti-apoptotic pathways. *Science* 2004;305:1163-7.
53. Wee P, Wang Z. Epidermal growth factor receptor cell proliferation signaling pathways. *Cancers (Basel)* 2017;9:52.
54. Gerritsen JS, Faraguna JS, Bonavia R, Furnari FB, White FM. Predictive data-driven modeling of C-terminal tyrosine function in the EGFR signaling network. *Life Sci Alliance* 2023;6:e202201466.
55. Chen N, Tyler LC, Le AT, Welsh EA, Fang B, Elliott A, et al. MIG6 mediates adaptive and acquired resistance to ALK/ROS1 fusion kinase inhibition through EGFR bypass signaling. *Mol Cancer Ther* 2024;23:92-105.
56. Lui VW, Peyser ND, Ng PK, Hritz J, Zeng Y, Lu Y, et al. Frequent mutation of receptor protein tyrosine phosphatases provides a mechanism for STAT3 hyperactivation in head and neck cancer. *Proc Natl Acad Sci U S A* 2014;111:1114-9.